Influence of Chain End and Molecular Weight on Molecular Motion of Polystyrene, Revealed by the ESR Selective Spin-Label Method

Yohei Miwa,[†] Takayuki Tanase,[†] Katsuhiro Yamamoto,[†] Masato Sakaguchi,[‡] Masahiro Sakai,[§] and Shigetaka Shimada*,[†]

Department of Material Science & Engineering, Nagoya Institute of Technology, Gokiso-cho, Showa-ku, Nagoya 466-8555, Japan; Nagoya Keizai University, 61 Uchikubo, Inuyama, 484-8503, Japan; and Research Center for Molecular-Scale Nanoscience, Institute for Molecular Science, 38 Nishigo-Naka, Myodaiji, Okazaki 444-8585, Japan

Received January 13, 2003

ABSTRACT: A local segmental mobility was determined by electron spin resonance (ESR) spin-label method for a series of polystyrene (PS) with various molecular weights. Each PS specimen was selectively spin-labeled with stable nitroxide radicals at a chain end or inside sites. Molecular motion at the inside of the chain was compared with that at the chain end from the temperature dependence of ESR spectra of the nitroxide radicals. The transition temperature of molecular motion, $T_{5.0mT}$, at which the extreme separation width due to ^{14}N anisotropic hyperfine splitting is 5.0 mT, increased with an increase in molecular weight. The WLF equation confirmed that the $T_{5.0mT}$ correlated with a glass transition temperature, T_g, of PS. The $T_{5.0mT}$ for the spin-labeled PS at the chain end was ca. 5 K lower than that for the spin-labeled PS at the inside sites due to the enrichment of the specific free volume around the chain end. The transition temperature, $T_{5.0mT}$, for both labeled PS depended on the molecular weight in accordance with the Unberreiter−Kanig equation for a glass transition. The $T_{5.0mT}$ for the spin-labeled PS at the chain end had a strong dependence on the molecular weight as compared with that at the inside sites because the molecular motion of the chain end was accelerated by an encounter of more than two chain ends. From the molecular weight dependence, we determined the short correlation time for segmental motion of the chain end, ca. 40 s, and the segment size undergoing the segmental motion at the T_g. The obtained segment size agreed well with the general segment size reported by others, 5−10 monomeric unit size.

Introduction

It is well-known that the glass transition temperature, T_g, of a given polymer is a function of its molecular weight.[1−3] Unberreiter and Kanig suggested the dependence of the T_g on number-average molecular weight (M_n) for polystyrene:[3]

$$1/T_g = 1/T_{g\infty} + A/M_n \quad (1)$$

Here, $T_{g\infty}$ is a value of the T_g at infinite molecular weight and A is a constant. On the assumption that the glass transition occurred at a constant value of the free volume fraction, they derived a theoretical expression of the same form as eq 1. In the derivation, they applied that a reduction of the molecular weight increases the number of chain ends per volume and, concomitantly, the free volume fraction. As a consequence, the glass transition temperature is depressed necessarily in order to reach the constant free volume fraction characteristic of the glass transition.

There has been great interest in the local segmental dynamics of polymer. The local segmental dynamics of polymer in solution has been reported by many authors.[4−7] They reported that the chain end had higher molecular mobility than other segments in the polymer solution. Here we raise additional questions. How different is the segmental motion in the region of the segments near chain ends from that of other segments in bulk? Does the increase in molecular weight affect on the rate of the segmental motion also in the region around the chain ends? To answer these questions, one has to observe the molecular mobility of the chain end distinguished from that of other segments. We have developed spin-label techniques in order to study the structure and dynamic behavior of polymer chains at a particular site or in a particular region.[8−16] When the nitroxide radical as a label of molecular motion is thermally and chemically stable, the temperature dependence of an ESR spectrum can be observed over a wide range of temperatures. Shimada et al. compared the molecular mobility at a polyethylene (PE) chain end with that at an inside segment of the PE chain through a spin-trapping method.[17] They reported that the molecular mobility of the chain end is higher than that of the inside segment of the chain. In this work, we selectively labeled at a PS chain end and an inside of the PS chain with a stable spin-label reagent.

The principal values of the anisotropic molecular g tensor and of the electron−nuclear hyperfine interaction tensor from the nitrogen nucleus ($I = 1$) are averaged out by the motion in the medium. Change in the line shape and in the separation between the outermost signals which appear in the ESR spectrum of the labels is measured as a function of temperature. The transition temperature at which the separation is 5.0 mT is defined as $T_{5.0mT}$, which correlated with the T_g.[18−20] In this paper, we compare the segmental motion of the chain end with that of the inside segment and discuss an influence of the molecular weight on the segmental motion of the chain end at the glass transition.

[†] Nagoya Institute of Technology.
[‡] Nagoya Keizai University.
[§] Institute for Molecular Science.

10.1021/ma030026l CCC: $25.00
Published on Web 04/10/2003

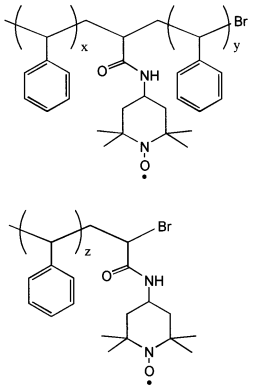

Figure 1. Chemical structure of spin-labeled PS at inside (above) and end (bottom) of chain.

Experimental Section

Material. Styrene (ST, Extra Pure Reagent, Nacalai Tesque Co., Ltd.), *tert*-butyl acrylate (*t*BA, Extra Pure Reagent, Tokyo Chemical Co., Ltd.), and toluene (Extra Pure Reagent, Nacalai Tesque) were distilled under reduced pressure. *N*,*N*,*N*′,*N*′,*N*″-Pentamethyldiethylenetriamine (PMDETA, 99%, Aldrich Chemical Co., Ltd.), 1-phenylethyl bromide (1-PEBr, 95%, Tokyo Chemical), CuBr (98%, Aldrich), and 2,2,6,6-tetramethyl-4-aminopiperidine-1-oxyl (4-amino-TEMPO, 99%, Aldrich) were used as received. Tetrahydrofuran (THF) and methanol were obtained from Nacalai Tesque Co., Ltd. (Extra Pure Reagent) and used without further purification.

Sample Preparation and Selective Spin-Labeling. 1. Chain End of PS (2 in Figure 1). All polymers were synthesized by atom transfer radical polymerization (ATRP) with CuBr/PMDETA complex and 1-PEBr as an initiator at 383 K.[21,22] *t*BA was incorporated to the isolated PS at the chain end via the ATRP technique. Nuclear magnetic resonance (NMR) was utilized to confirm the attachment of the *t*BA to the PS chain end. The yield of *t*BA attached at one chain end of the PS was calculated using the M_n of the PS determined by gel permeation chromatography (GPC) and the ratio of protons of the *tert*-butyl group of the *t*BA to that of a benzene ring of the PS. It was confirmed that three *t*BA were attached for ten PS chains. The selective spin-label at the chain end was carried out by amide−ester interchange reaction between the *tert*-butyl moiety of the chain end and 4-amino-TEMPO in toluene at 283 K for 4 days. The chain end-labeled PS was precipitated from toluene/THF solution to a water/methanol mixture, was filtered to remove a large amount of unreacted spin-label reagents, and was dried in a vacuum at 373 K for 24 h. This procedure was repeated more than four times to completely remove the unreacted spin-label reagents.

2. Inside of PS Chain (1 in Figure 1). Poly(S-*random*-*t*BA) was obtained by random copolymerization of ST and *t*BA using the ATRP technique.[23] Poly(S-*random*-*t*BA) was characterized by NMR, and the initial molar composition of ST: *t*BA = 98:2. The *tert*-butyl moieties in poly(S-*random*-*t*BA) were reacted with 4-amino-TEMPO. The sample was purified by the same procedure in the case of the end spin-labeled PS.

The spin-labeled PS's were analyzed by GPC to determine the molecular weight and its distribution. The PS's had a narrow molecular weight distribution, M_w/M_n, ranging from 1.07 to 1.25.

Measurement. NMR was performed on a Bruker AVANCE 200 spectrometer using deuterated chloroform at 298 K with tetramethylsilane as an internal reference.

The M_n and M_w/M_n of the PS were determined by GPC in THF (1 mL/min) at 313 K on four polystyrene gel columns (Tosoh TSK gel GMH (beads size is 7 μm), G4000H, G2000H, and G1000H (5 μm)) that were connected to a Tosoh CCPE (Tosoh) pump and an ERC-7522 RI refractive index detector (ERMA Inc.). The columns were calibrated against standard polystyrene (Tosoh) samples.

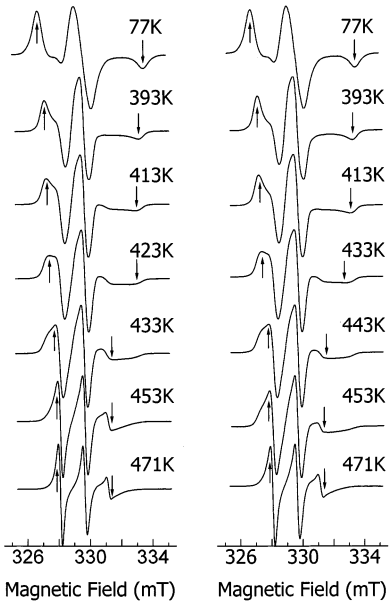

Figure 2. Temperature-dependent ESR spectra of spin-labeled PS at chain end (left, M_n = 21K) and at inside site (right, M_n = 22K). Separation between arrows shows extreme separation width.

Each sample was contained in a quartz tube, and the tube was depressurized to a pressure of 10^{-4} Torr and sealed before ESR measurement. ESR spectra at 77 K and higher temperatures were observed at low microwave power level to avoid power saturation and with 100 kHz fielded modulation using JEOL JES-FE3XG and JES-RE1XG spectrometers (X band) coupled to microcomputers (NEC PC-9801). The signal of 1,1-diphenyl-2-picrylhydrazyl (DPPH) was used as a *g* tensor standard. The magnetic field was calibrated with the well-known splitting constants of Mn^{2+}.

A modulated temperature differential scanning calorimeter (MDSC, TA 5000) manufactured by TA Instruments was used. A modulation amplitude of 1.5 K and a period of 60 s were used at a heating rate of 2 K/min. The calorimeter was calibrated with an indium standard.

Results and Discussion

ESR spectra of the spin-labeled PS at the chain end (M_n = 21K) and the inside sites (M_n = 22K) in the temperature range 77−471 K are shown in Figure 2. In general, the outermost splitting width of the main triplet spectrum due to hyperfine coupling caused by the nitrogen nucleus narrows with an increase in mobility of the radicals because of motional averaging of the anisotropic interaction between an electron and a nucleus. The complete averaging gives rise to the isotropic narrowed spectrum. The extreme separation width between arrows shown in Figure 2 gradually narrows and steeply drops with an increase in the temperature. The temperature dependence of the extreme separation width for each specimen is shown in Figure 3. The steep drop is caused by a micro-Brownian type molecular motion.[24−26] We estimated a transition temperature of molecular motion, $T_{5.0mT}$, at which the extreme separation width is equal to 5.0 mT. The $T_{5.0mT}$'s of the spin-labeled PS at the chain end ($T_{5.0mT,e}$) and the inside sites ($T_{5.0mT,i}$) are 423 and 435 K, respectively. The $T_{5.0mT}$ of the spin-labeled PS at the chain end is lower than that of the spin-labeled PS at the inside site. It can be considered that the high mobility of the chain ends is caused by the large free volume at the chain end in comparison with that at the

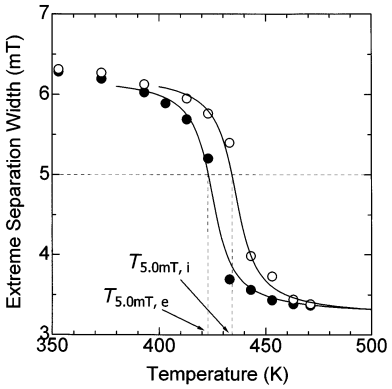

Figure 3. Temperature dependence of extreme separation width for spin-labeled PS at chain end (solid) and inside site (open).

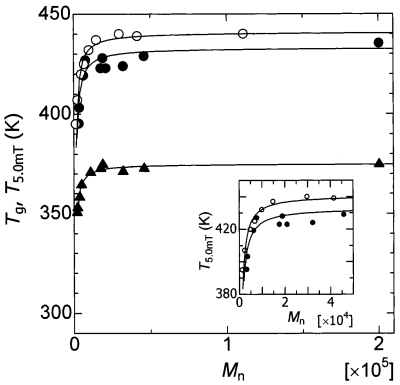

Figure 4. Plots of $T_{5.0mT,e}$ (solid circle), $T_{5.0mT,i}$ (open circle), and $T_{g,DSC}$ (triangle) vs M_n.

inside of the chain. Many authors have reported that the chain ends bring an incremental amount of the free volume over segments; as a result, the glass transition temperature is depressed.[1−3] Recently, Kajiyama and co-workers reported that the polymer surface enriched with segregated chain ends exhibited higher molecular mobility.[27−30] The transition temperature, $T_{5.0mT}$, appears at higher temperature than the T_g of PS because of a higher frequency corresponding to the rate of averaging of the anisotropic hyperfine splitting.[24−26] The T_g of the PS estimated from thermal analysis, $T_{g,DSC}$, was obtained from MDSC curves on heating at a rate of 2.0 K/min. The $T_{g,DSC}$ was taken to be the midpoint, i.e., the temperature corresponding to half of the endothermic shift. The $T_{g,DSC}$, $T_{5.0mT,e}$, and $T_{5.0mT,i}$ were plotted against M_n in Figure 4. The most successful relationship of temperature dependence for the viscous flow, viscoelastic response, and dielectric dispersion of polymers and supercooled liquids is the Williams−Landel−Ferry (WLF) equation[31]

$$\log a_T = \log(\tau(T)/\tau(T_0)) = -C_1(T - T_0)/(C_2 + T - T_0) \quad (2)$$

where a_T is called the shift factor, τ is a relaxation time, T_0 is the chosen reference temperature, and C_1 and C_2 are universal constants. The $T_{g,DSC}$ and $T_{5.0mT}$ were adopted as T_0 and T, respectively. When T_0 is chosen to be T_g, the constants C_1^g and C_2^g are universal values of 17.44 and 51.6, respectively. The relaxation time of 7×10^{-9} s[19] and 100 s[32,33] were substituted in $\tau(T)$ and $\tau(T_0)$, respectively. The ΔT (= $T_{5.0mT} - T_{g,DSC}$) was calculated to be 72 K from eq 2. The ΔT ($T_{5.0mT\infty,i} -$

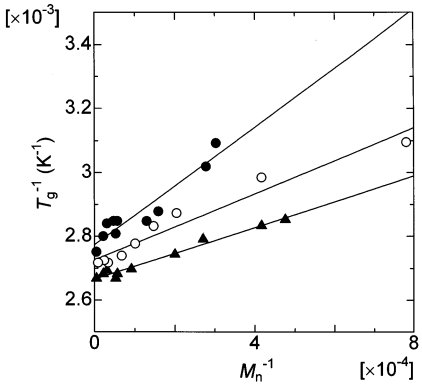

Figure 5. Molecular weight dependence of $T_{g,e}$ (solid circle), $T_{g,i}$ (open circle), and $T_{g,DSC}$ (triangle) for monodisperse PS. Solid lines present eq 1 for all data with $T_{g\infty}$, e = 361 K, A_e = 0.920, $T_{g\infty,i}$ = 366 K, A_i = 0.518, $T_{g\infty,DSC}$ = 375 K, and A_{DSC} = 0.404.

$T_{g\infty,DSC}$) obtained from the experiments, 66 K, agreed well with the calculated value, 72 K. The experimental temperature, $T_{5.0mT\infty,i}$, is adopted as an asymptotic value in infinite molecular weight for the $T_{5.0mT,i}$ in Figure 4. The $T_{5.0mT,e}$ and $T_{5.0mT,i}$ were reduced to transition temperatures, $T_{g,e}$ and $T_{g,i}$, for τ = 100 s by the WLF equation.

The inverse of the $T_{g,DSC}$, $T_{g,e}$, and $T_{g,i}$ was plotted against reciprocal of the M_n as shown in Figure 5. From the linear relationship of eq 1, the $T_{g\infty,DSC}$ and A_{DSC} were determined to be 375 K and 0.404, respectively. The $T_{g\infty,i}$ and A_i were also estimated to be 366 K and 0.518, respectively. The slight differences, $T_{g\infty,DSC} - T_{g\infty,i}$ and $A_{DSC} - A_i$, are caused by the ambiguity of the C_1 and C_2 in the WLF equation which is used for the calculation of the $T_{g,i}$, as mentioned previously. Anyhow, the similar relations of the transition temperature against the M_n demonstrate that the $T_{5.0mT}$ for the inside label correlates with the T_g, namely, α relaxation of PS. The molecular weight dependence of the $T_{g,e}$ was also in good agreement with eq 1. The $T_{g\infty,e}$ and A_e were 361 K and 0.920, respectively. The $T_{g\infty,e}$ was 5 K lower than the $T_{g\infty,i}$. The value of the A_e is roughly 2 times larger than the A_i and A_{DSC}. As mentioned previously, the chain end has higher molecular mobility than the inside segment due to the larger free volume around the chain end than that around the inside segment. The strong molecular weight dependence of the $T_{g,e}$ demonstrated that the $T_{5.0mT,e}$ also reflected the α relaxation of the PS because the local mode β and γ relaxation's of the PS have no molecular weight dependence. These results indicate that the molecular mobility of the chain end can be also interpreted in terms of the free volume fraction which is affected by the surrounding segments. This behavior was caused by the cooperative motion of the chain end with the surrounding segments at the glass transition. It is well-known that the glass transition occurs on the basis of the cooperative motion between neighboring segments. A certain segment of a polymer in bulk is tightly meshed by neighboring segments like a group of engaging gears below the T_g. In this condition, a cooperative motion with the neighboring segments is necessary for the segments to undergo the rotational relaxation. We considered that the $T_{g,e}$ showed the molecular weight dependence because the chain end segment also moved cooperatively with the neighboring segments at the glass transition. Even if experimental errors are taken into account, the A_e (=0.920) is much bigger than the A_i (=0.518). This result indicates that

the $T_{g,e}$ has a strong dependence on the molecular weight as compared with the $T_{g,i}$. This behavior is instructive to understand the relationship between the free volume and the molecular motion. Freed et al.[34] and Kivelson[35] studied the segmental rotational motion in polymer chains by the ESR technique. Shimada et al. compared the correlation time, τ_c, for the segmental rotational motion of the chain end with that of the inside segment of the PE using Kivelson's equation.[17] Shimada et al. reported that the τ_c of the chain end was shorter than that of the inside segment of the PE. In this paper, we discuss the difference between the τ_c's of specific sites of the PS in terms of the averaged relaxation time calculated from the probability of the encounter of the labeled segments as following model. We assumed that one segment is surrounded with four other segments. The combination of an arrangement of each segment in this situation was considered. First, for simplicity, a degree of polymerization was used as the number of the motional segment of the PS; i.e., the segment was represented as a monomer unit. Four surrounding segments in the model consist of four polymeric chains including eight end segments. We take a segment surrounded with four segments of its own and other polymer chains. The total number of the combination in order for the four segments to be arranged is

$$N(N-1)(N-2)(N-3)/4! \tag{3}$$

where $N = 4n$, n being the degree of polymerization of the PS. When the four segments are the inside segments, the number of its combination (denoted as i_4) is

$$(N-8)(N-9)(N-10)(N-11)/4! \tag{4}$$

The number of the combination composed by three inside segments and one chain end segment (denoted as i_3e_1) is

$$8[(N-8)(N-9)(N-10)/3!] \tag{5}$$

Similarly, the number of the other combinations is

$$[(N-8)(N-9)/2!][(8\times 7)/2!] \quad \text{for } i_2e_2 \tag{6}$$

$$(N-8)[(8\times 7\times 6)/3!] \quad \text{for } i_1e_3 \tag{7}$$

$$(8\times 7\times 6\times 5)/4! \quad \text{for } e_4 \tag{8}$$

When the n is large, the probability that the noticed segment is surrounded with four inside segments, eq 4/eq 3 is reduced to be $\{1 - 9.5/n\}$. In the same manner, the probability that the noticed segment is surrounded by three inside and one end segments, eq 5/eq 3, is $8/n$. Other probabilities eq 6/eq 3, eq 7/eq 3, and eq 8/eq 3 can be ignored. The Doolittle equation is the most relevant to relate a relaxation rate to a free volume, V_f.

$$1/\tau_c = A\exp(-B/V_f)$$

Here, A and B are constants. The average relaxation rate is considered to be expressed by

$$\ln(1/\tau_c) = \sum_k P_k(1/V_{f,k}), \quad \sum_k P_k = 1$$

P_k and $V_{f,k}$ are the probability and the local free volume of each arrangement, respectively. Therefore, the average relaxation rates for end and inside segments are represented as following equations:

$$\ln(1/\tau_e) = \sum_k P_{e,k}\ln(1/\tau_{e,k}), \quad \sum_k P_{e,k} = 1$$

for the end segment

$$\ln(1/\tau_i) = \sum_k P_{i,k}\ln(1/\tau_{i,k}), \quad \sum_k P_{i,k} = 1$$

for the inside segment.

$P_{e,k}$ and $P_{i,k}$ are the probabilities of each arrangement for end and inside segments, respectively. Therefore, when the chain end segment is surrounded with four segments, the average segmental rotational rate ($1/\tau_e$) of the chain end spin-labeled PS at the glass transition temperature is

$$\ln(1/\tau_e) = (1-9.5/n)\ln(1/\tau_{e-i_4}) + (8/n)\ln(1/\tau_{e-i_3e_1})$$

$$= [8\ln(1/\tau_{e-i_3e_1}) - 9.5\ln(1/\tau_{e-i_4})]/n + \ln(1/\tau_{e-i_4}) \tag{9}$$

Here the $1/\tau_{e-i_4}$ is the segmental rotational rate of the chain end segment when the chain end segment is surrounded with four inside segments. The $1/\tau_{e-i_3e_1}$ means the segmental rotational rate of the chain end segment surrounded with three inside segments and one chain end segment. Similarly, the segmental rotational rate ($1/\tau_i$) of the inside spin-labeled PS at the glass transition temperature is expressed by

$$\ln(1/\tau_i) = (1-9.5/n)\ln(1/\tau_{i-i_4}) + (8/n)\ln(1/\tau_{i-i_3e_1})$$

$$= [8\ln(1/\tau_{i-i_3e_1}) - 9.5\ln(1/\tau_{i-i_4})]/n + \ln(1/\tau_{i-i_4}) \tag{10}$$

The $\ln(1/\tau_e)$ and $\ln(1/\tau_i)$ obtained from the experiment was plotted against the reciprocal of the n in Figure 6, where the τ_e and τ_i were calculated using the WLF equation with the reference temperature of 366 K. The data were fitted with eqs 9 and 10 for the chain end and the inside site by least-squares method, respectively. The τ_{e-i_4} and τ_{i-i_4} are estimated to be 37 and 91 s from the intercept terms of the fitted lines in Figure 6, respectively. It is very interesting that the shorter relaxation time of the segmental motion at the chain end sites can be obtained. In general, one considers that the motional segment size is bigger than the monomer size. Kusumoto et al. and Bullock et al. estimated the motional segment size at the T_g using the ESR.[26,36] They reported that the order of 5−10 monomeric units was involved in the segmental motion. Here, the number of

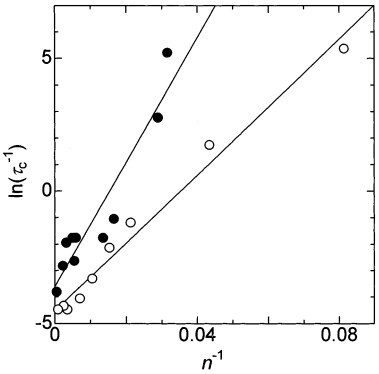

Figure 6. Influence of degree of polymerization on $\ln(1/\tau_e)$ (solid) and $\ln(1/\tau_i)$ (open). $\ln(1/\tau_e)$ and $\ln(1/\tau_i)$ are fitted with $\ln(1/\tau_e) = 235/n - 3.6$ and $\ln(1/\tau_i) = 128/n - 4.5$ obtained by the least-squares method.

the motional segment per one PS chain, n', is given by $n' = n/x$, where x is the number of monomer units involved in the segmental motion at the T_g. Then the n' should be substituted into the n in eqs 9 and 10. When it is assumed that the $\tau_{i-i_3e_1}$ is comparable with the τ_{e-i_4}, the x is estimated to be nine from the slope of the fitted curve using eq 10. This result implies that approximately nine monomeric units size segment undergoes a segmental motion at the T_g. The estimated size of the motional segment agrees well with the 5−10 monomer units reported by Kusumoto. When it is assumed that the x of the chain end segment is equal to that of the inside segment, the $\tau_{e-i_3e_1}$ is obtained to be 2.8 s from the slope of the fitted line with eq 9. The relaxation time of the segmental rotation at the region containing two chain ends, $\tau_{e-i_3e_1}$ (= 2.8 s), is much shorter than that containing one chain end, τ_{e-i_4} (= 37 s). This is induced by the much larger free volume generated by two chain ends. A decrease in the molecular weight leads to an increase in the number of chain ends. As a result, the probability of the encounter of two chain ends increases. As the molecular weight decreases, the T_g in the region near the chain end is steeply depressed. The result of this work will be important to reveal the local transition temperature of polymer materials. For example, Kajiyama et al. compared the molecular weight dependence of the T_g of polymer surface to that of the bulk.[29,37] They reported that the polymer surface enriched with segregated chain ends exhibit higher molecular mobility. As the molecular weight decreased, the T_g of the polymer surface was steeply depressed as compared to that of the bulk. They concluded that this behavior might be caused by the effect of the increased free volume at the surface due to a preferential surface enrichment of chain end groups. From the result of our present work, we suppose that the main factor of the strong dependence of the molecular weight on the surface T_g is arising from the probability of the encounter of more than two chain ends.

Conclusion

A comparison of the segmental motion of the chain end with that of inside sites of the PS was successful by the ESR measurements with the selective spin-label method. The $T_{g\infty,e}$ was ca. 5 K lower than the $T_{g\infty,i}$ due to the large free volume around the chain end group as compared to the inside of the PS chain. Not only the $T_{g,i}$ but also the $T_{g,e}$ showed the molecular weight dependence because of the cooperative motion of the chain end with surrounding segments at the glass transition. The relaxation time of the specific region of the PS was estimated from the molecular weight dependence of the combination of the chain end and inside segments, and it was revealed that the encounter of more than two chain ends brought the steep decrease in the τ_c. In conclusion, the ESR selective spin-label method revealed the relationship between the local free volume fraction and the local molecular mobility.

Acknowledgment. Thanks are due to the Research Center for Molecular Materials, the Institute for Molecular Science, for assistance in obtaining the MDSC data. This research was carried out with a grant from the NITECH 21st Century COE Program for Environmental Ceramics.

References and Notes

(1) Fox, T. G.; Flory, P. J. *J. Appl. Phys.* **1950**, *21*, 581.
(2) Beevers, R. B.; White, E. F. T. *Trans. Faraday Soc.* **1960**, *56*, 117.
(3) Unberreiter, K.; Kanig, G. *J. Colloid Sci.* **1952**, *7*, 569.
(4) Waldow, D. A.; Ediger, M. D.; Yamaguchi, Y.; Matsushita, Y.; Noda, I. *Macromolecules* **1991**, *24*, 3147.
(5) Spyros, A.; Dais, P.; Heatley, F. *Macromolecules* **1994**, *27*, 6207.
(6) Glowinkowski, S.; Gisser, D. J.; Ediger, M. D. *Macromolecules* **1990**, *23*, 3520.
(7) Adolf, D. B.; Ediger, M. D.; Kitano, T.; Ito, K. *Macromolecules* **1992**, *25*, 867.
(8) Shimada, S.; Hori, Y.; Kashiwabara, H. *Macromolecules* **1985**, *18*, 170.
(9) Hori, Y.; Makino, Y.; Kashiwabara, H. *Polymer* **1984**, *25*, 1436.
(10) Shimada, S.; Hori, Y.; Kashiwabara, H. *Macromolecules* **1988**, *21*, 979.
(11) Shimada, S.; Watanabe, T. *Polymer* **1998**, *39*, 1703.
(12) Shimada, S.; Horiguchi, K.; Yamamoto, K. *Colloid Polym. Sci.* **1998**, *276*, 412.
(13) Shimada, S.; Sugimoto, A.; Kawaguchi, M. *Polymer* **1997**, *38*, 2251.
(14) Shimada, S.; Watanabe, T. *Polymer* **1998**, *39*, 1711.
(15) Shimada, S.; Hane, Y.; Watanabe, T. *Polymer* **1997**, *38*, 4667.
(16) Shimada, S.; Maruta, A.; Yamamoto, K. *Polym. J.* **2000**, *32*, 1038.
(17) Kitahara, T.; Shimada, S.; Kashiwabara, H. *Polymer* **1980**, *21*, 1299.
(18) *Molecular Motion in Polymers by ESR*; Boyer, R. F., Keinath, S. E., Eds.; Harwood Academic: New York, 1980.
(19) Törmälä, P.; Weber, G. *Polymer* **1978**, *19*, 1026.
(20) Schlick, S.; Harvey, R. D.; Alonso-Amigo, M. G.; Klempner, D. *Macromolecules* **1989**, *22*, 822.
(21) Patten, T. E.; Xia, J.; Abernathy, T.; Matyjaszewski, K. *Science* **1996**, *272*, 866.
(22) Matyjaszewski, K.; Patten, T. E.; Xia, J. *J. Am. Chem. Soc.* **1997**, *119*, 674.
(23) Ziegler, M. J.; Matyjaszewski, K. *Macromolecules* **2001**, *34*, 415.
(24) Shimada, S.; Kashima, K. *Polym. J.* **1996**, *28*, 690.
(25) Sohma, J.; Sakaguchi, M. *Adv. Polym. Sci.* **1978**, *20*, 109.
(26) Kusumoto, N.; Sano, S.; Zaitsu, N.; Motozato, Y. *Polymer* **1976**, *17*, 448.
(27) Xie, F.; Zhang, H. F.; Lee, F. K.; Du, B.; Tsui, O. K. C.; Yokoe, Y.; Tanaka, K.; Takahara, A.; Kajiyama, T.; He, T. *Macromolecules* **2002**, *35*, 1491.
(28) Tanaka, K.; Taura, A.; Ge, S.; Takahara, A.; Kajiyama, T. *Macromolecules* **1996**, *29*, 3040.
(29) Kajiyama, T.; Tanaka, K.; Takahara, A. *Macromolecules* **1997**, *30*, 280.
(30) Tanaka, K.; Jiang, X.; Nakamura, K.; Takahara, A.; Kajiyama, T.; Ishizoe, T.; Hirao, A.; Nakahama, S. *Macromolecules* **1998**, *31*, 5148.
(31) Williams, M. L.; Landel, R. F.; Ferry, J. D. *J. Am. Chem. Soc.* **1995**, *77*, 3701.
(32) Angell, C. A. *J. Non-Cryst. Solids* **1991**, *131−133*, 13.
(33) Ngai, K. L.; Plazek, D. J. *Rubber Chem. Technol.* **1995**, *68*, 376.
(34) Goldman, S. A.; Bruno, G. V.; Freed, J. H. *J. Phys. Chem.* **1972**, *76*, 1858.
(35) Kivelson, D. *J. Chem. Phys.* **1960**, *33*, 1094.
(36) Bullock, A. T.; Cameron, G. G.; Miles, I. S. *Polymer* **1982**, *23*, 1536.
(37) Satomi, N.; Takahara, A.; Kajiyama, A. *Macromolecules* **1999**, *32*, 4474.

MA030026L